Available online at www.sciencedirect.com
ScienceDirect
Ceramics International 38S (2012) S237–S240
CERAMICS INTERNATIONAL
www.elsevier.com/locate/ceramint

Fabrication and characterization of high curie temperature $BiSc_{1/2}Fe_{1/2}O_3$–$PbTiO_3$ piezoelectric films by a sol–gel process

Caifu Zhong, Xiaohui Wang *, Longtu Li *

State Key Laboratory of New Ceramics and Fine Processing, Department of Materials Science and Engineering, Tsinghua University, Beijing 100084, China

Available online 4 May 2011

Abstract

$(1-x)BiSc_{1/2}Fe_{1/2}O_3$–$xPbTiO_3$ (BSF–PT) thin films with the composition of $x = 0.45$–0.6 were fabricated on the Pt(1 1 1)/Ti/SiO_2/Si substrates via an aqueous sol–gel method. The structure and electric properties of these BSF–PT thin films were investigated. The films showed a maximum dielectric and piezoelectric activities for $x = 0.55$ which was around the morphotropic phase boundary (MPB) composition in BFS–PT ceramics. The local effective piezoelectric coefficient d_{33}^* of the BSF–PT film for $x = 0.55$ was approximately 50 pm/V, which was comparable to that of the $BiScO_3$–$PbTiO_3$ (BSPT) thin films, and the curie temperature was about 420 °C, also similar to that of BSPT films, but higher than that of PZT thin films. Therefore, the relative low cost of the BFS–PT films compared with that of BSPT films suggests potential device applications in high temperature.

Keywords: A. Films; C. Piezoelectric properties; High curie temperature; $Bi(Sc,Fe)O_3$–$xPbTiO_3$

1. Introduction

Ferroelectric thin films have been intensively studied in recent years for their application in nonvolatile ferroelectric random access memories, microelectromechanical systems and high frequency electrical components [1–3]. Though much intention has been focused on the lead zirconate titanate (PZT) systems due to their large piezoelectric displacement and permanent polarization [4], the relative low curie temperature *Tc* (usually lower than 386 °C for PZT) limits their applications in automotive, aerospace and other areas that require high temperature stability of the materials. Eitel et al. [5,6] reported a new perovskite system $BiScO_3$–$PbTiO_3$ (BSPT), which exhibited a high *Tc* of 450 °C and comparable ferroelectric and piezoelectric properties to those of PZT at the morphotropic phase boundary (MPB). As the raw material of Sc is very expensive, a substituent for Sc_2O_3 is required to reduce the cost of raw material. Therefore, $(1-x)BiSc_{1-y}Fe_yO_3$–$xPbTiO_3$ (BFS–PT) solid solutions were fabricated and investigated, and for $y = 0.5$, BFS–PT ceramics with the MPB compositions ($x = 0.5$–0.55) showed a piezoelectric coefficients (d_{33}) of 300 pC/N, which was similar to that of hard PZT composition, but a curie temperature at ~440 °C that was about 60 °C higher [7,8].

Of these compositions, polycrystal BSPT thin films had been grown on platinized silicon substrates via sol–gel method [9,10], epitaxial BSPT thin films were prepared on (1 0 0) $SrRuO_3$/(1 0 0) $LaAlO_3$ single crystal substrates via pulsed laser deposition [11], and subsequently on Nb-doped $SrTiO_3$ (1 0 0) single crystal substrates via sol–gel method in our previous studied [12]. However, reports on piezoelectric properties and high temperature characteristic of the BFS–PT thin films were few. Thus, in this paper, the structure and electric properties of BFS–PT thin films fabricated by chemical solution deposition are investigated.

2. Experimental

Lead acetate [$Pb(COOCH_3)_2$], tetrabutyl titanate [$Ti(OC_4H_9)_4$], scandium acetate [$Sc(COOCH_3)_3$], bismuth nitrate [$Bi(NO_3)_3$], and iron nitrate [$Fe(NO_3)_3$] were chosen as the raw materials with glacial acetic acid, isopropyl alcohol and distilled water as the solvents. The preparation details of the $(1-x)BiSc_{1/2}Fe_{1/2}O_3$–$xPbTiO_3$ precursor solutions were similar to that of BSPT precursors described elsewhere [13].

* Corresponding authors. Tel.: +86 10 62792689; fax: +86 10 62792689.
E-mail addresses: wxh@mail.tsinghua.edu.cn (X. Wang), lltdms@mail.tsinghua.edu.cn (L. Li).

0272-8842/$36.00 © 2011 Published by Elsevier Ltd and Techna Group S.r.l.
doi:10.1016/j.ceramint.2011.04.091

Four solutions in the proportions of x =0.6, 0.55, 0.5, 0.45 with 10% lead excess were synthesized. The thin films were first deposited onto Pt(1 1 1)/Ti/SiO_2/Si(1 1 1) substrates by spin coating at 5000 rpm for 30 s, then dried at 100 °C and pyrolyzed at 400 °C in ambient atmosphere. This process was repeated for 10 times to obtain a desired thickness (~400 nm) for the BFS–PT films. Subsequently these films were annealed at 700 °C. All the heating treatments were carried out by a rapid thermal processing furnace. Top electrodes of platinum, 0.2 mm in diameter, were sputtering deposited onto the surface of the BSPT thin films for electric properties measurements.

The crystal structures were characterized by using a high resolution X-ray diffractometer (XRD, 2500, Rigaku, Japan) with a monochromator. A scanning probe microscopy system (SPM, SPI4000&SPA300HV, Seiko, Tokyo, Japan), was employed to observe the surface morphologies of the BFS–PT thin films, and the measurements were carried out at the dynamic force microscopy (DFM) mode. A ferroelectric test module (TF 2000 analyzer, axiACCT, Aachen, Germany) and a precision LCR Meter (4980A, Agilent, USA) were employed to evaluate the ferroelectric and dielectric properties of the samples. The curie temperatures of the BFS–PT thin films were investigated by the LCR Meter (4980A) in combination with a temperature control system. The effective piezoelectric coefficients d_{33}^* were measured by the SPM with a conductive Rh-coated Si cantilever. Prior to measurement of the effective d_{33}^* coefficients, a dc voltage was applied to the aim area at room temperature for poling.

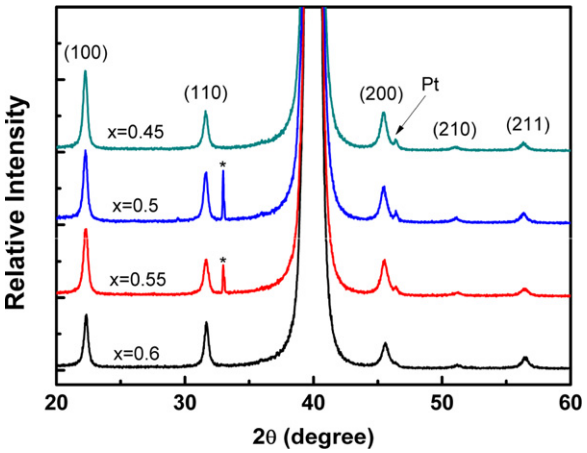

Fig. 1. XRD patterns for the sol–gel derived BFS–PT thin film with different compositions. *: Unexpected peaks from the substrate.

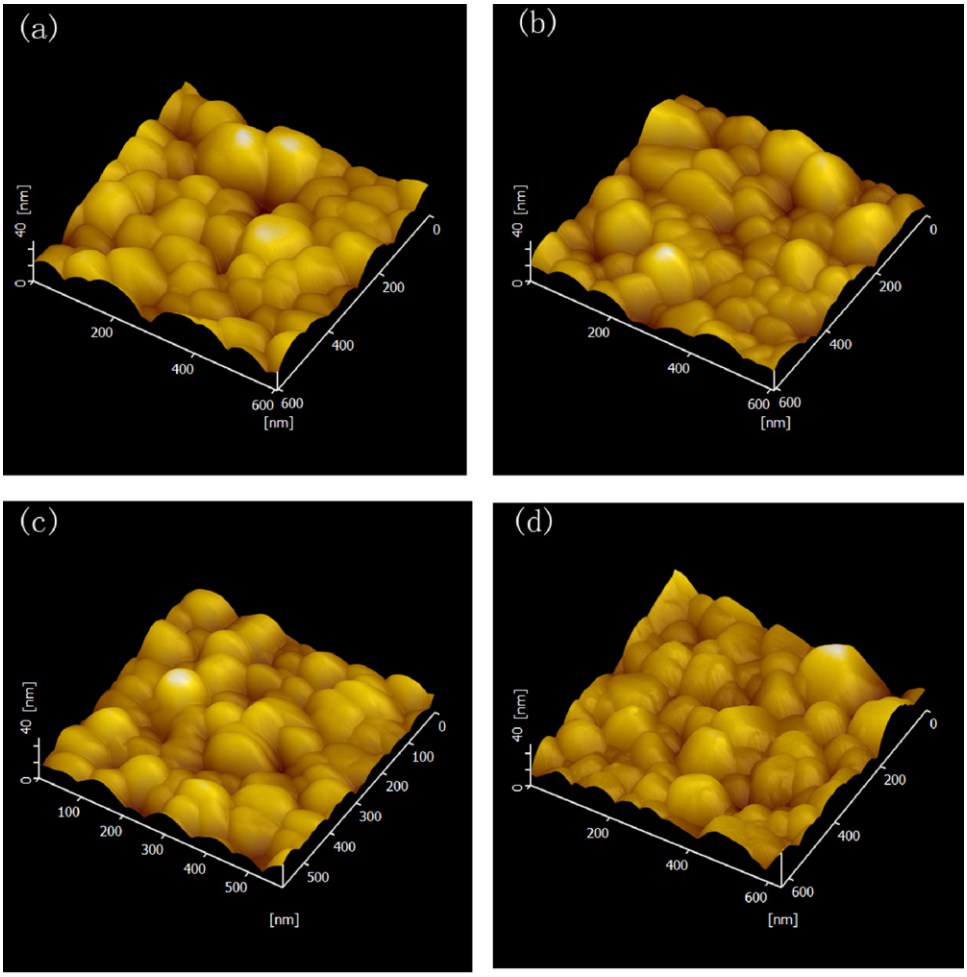

Fig. 2. Surface microstructure of the BFS–PT films with different compositions observed by DFM (a) $x = 0.6$, (b) $x = 0.55$, (c) $x = 0.5$, (d) $x = 0.45$.

3. Results and discussion

Fig. 1 shows the XRD patterns of the sol–gel derived BFS–PT thin films with different compositions. For all patterns, pure perovskite phases are obtained without any second phases such as pyrochlore existing to the detection limits of our diffractometer. No coexistent peaks of tetragonal phase and rhombohedral phase have been found for all films, suggesting a solid-solution phase is formed at the composition range. The surface morphologies of these BFS–PT thin films with different compositions measured by DFM are displayed in Fig. 2. All films exhibit similar surface grain structures and grain size distributions, and the mean grain size of all these films are about 75 nm.

Fig. 3 presents the ferroelectric hysteresis loops measured at 100 Hz for the BFS–PT thin films. All of the samples show well saturated hysteresis loops with high direct current (DC) resistivity, which indicates few defects existing in the sol–gel derived BFS–PT thin films. It is found that the highest remanent polarization (Pr) is obtained at $\sim$35 μC/cm^2 for $x = 0.55$, and the coercive field (Ec) values for all these films are similar, about 110 kV/cm. The Pr values measured here are comparable with that we reported in our previous work for the BSPT films [9].

The DC bias dependence of the dielectric constant for these BFS–PT thin films, measured under a small oscillation signal of 0.5 V at 1 kHz, is displayed in Fig. 4. Typical ferroelectric butterfly loops are observed in all the samples. The dielectric loss of these thin films, not shown in the figure, present a similar value of about 0.05. Besides, as shown in the inset, the relative dielectric constant reaches the maximum value around the MPB compositions of $x = 0.55$, which is consistent with results in bulk BSF–PT materials. For ferroelectric films, the contributions to the permittivity can be divided into intrinsic and extrinsic component [14]. The extrinsic contribution which mainly originated from the domain wall motion will be restricted by the direct current bias field when the field is larger than the coercive field [14]. The permittivity values for the BFS–PT films with different compositions in the figure become more and more similar as the DC bias field increases, thus we can propose that the intrinsic permittivity exhibits a weak relationship with the composition and the enhanced dielectric properties at MPB composition may be attributed to the extrinsic contribution which is mainly originated from the reversible domain wall motion.

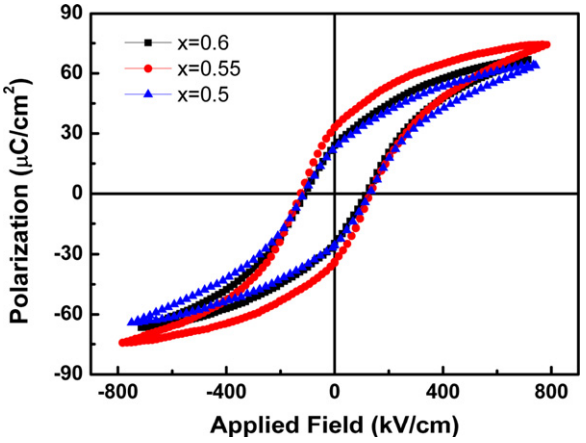

Fig. 3. Ferroelectric hysteresis loops for the BFS–PT films with different compositions.

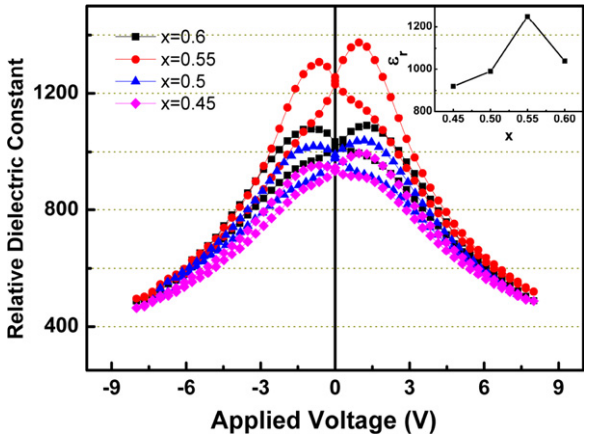

Fig. 4. DC bias voltage dependence of the dielectric constant of the sol–gel derived BFS–PT films with different compositions, the inset shows the quasi-static dielectric permittivity dependence on the composition.

The temperature dependence of the dielectric constant and loss measured at 100 kHz for the BFS–PT films is shown in Fig. 5. The permittivity peak of the films in the curve is strongly flatten and broaden compared with that in ceramics [7], and the curie temperatures of BFS–PT films for $x = 0.6$, 0.55, 0.5 are about 440 °C, 420 °C, 405 °C, respectively, which are all slightly lower than that observed in BFS–PT ceramics with the same composition [7]. The broaden of permittivity peak may attribute to the effect of the small grain size, silimar phenomenon has been reported for BSPT ceramics [15] and $BaTiO_3$ ceramics [16].

The piezoelectric properties of the BFS–PT thin films are shown in Fig. 6. All these three samples exhibit typical ‘‘butterfly’’ shape displacement-voltage loops. The thin films present the largest displacement for samples with the MPB composition of $x = 0.55$, and the effective piezoelectric coefficient d^*_{33} can be calculated from the displacement-voltage loops, which are about 42 pm/V, 50 pm/V and 40 pm/V

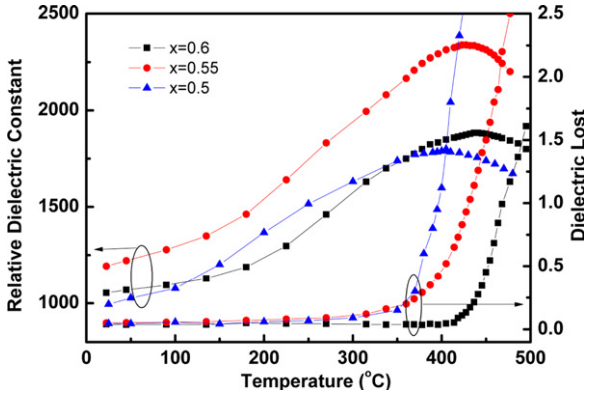

Fig. 5. The dielectric properties of the BFS–PT films with different compositions as a function of temperature.

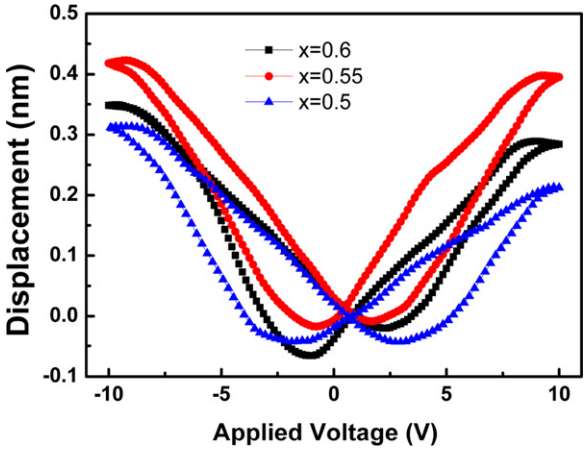

Fig. 6. The piezoelectric displacement – voltage loops for the sol–gel derived BFS–PT films with different compositions.

for $x = 0.6$, $x = 0.55$, $x = 0.5$, respectively. The results of piezoelectric properties are consistent with the dielectric results, indicating that the enhancement of the piezoelectric activity around MPB composition may also be attributed to the larger activity of domain wall motion. However, it needs further investigation to be proved.

4. Conclusion

$(1 - x)BiSc_{1/2}Fe_{1/2}O_3$–$xPbTiO_3$ ($x = 0.45$–0.6) thin films were successfully fabricated via sol–gel process. The films exhibited a maximum dielectric and piezoelectric activity at $x = 0.55$ which was around the MPB composition ($x = 0.5$–0.55 in ceramics), and the higher mobility of domain wall was supposed to be the main reason for the enhanced dielectric and piezoelectric properties. The high *Tc* temperature (∼420 °C for $x = 0.55$), comparable piezoelectric properties with respect to BSPT films, and lower cost of the BFS–PT thin films indicate that it is suitable for high temperature device applications.

Acknowledgements

The work was supported by National Science fund for distinguished young scholars (Grant No. 50625204), Science Fund for Creative Research Groups (Grant No. 50921061), and by the Ministry of Sciences and Technology of China through National Basic Research Program of China (973 Program 2009CB623301), outstanding tutors for doctoral dissertations of S&T project in Beijing (No. YB20081000302), and by Tsinghua University Initiative Scientific Research Program.

References

[1] J.F. Scott, C.A.P. Dearaujo, Ferroelectric memories, Science 246 (1989) 1400–1405.
[2] M. Dawber, K.M. Rabe, J.F. Scott, Physics of thin-film ferroelectric oxides, Reviews of Modern Physics 77 (2005) 1083–1130.
[3] N. Setter, D. Damjanovic, L. Eng, G. Fox, S. Gevorgian, S. Hong, A. Kingon, H. Kohlstedt, N.Y. Park, G.B. Stephenson, Ferroelectric thin films: review of materials, properties, and applications, Journal of Applied Physics 100 (2006) 051606.
[4] W.R Cook, J.R. Jaffe, Piezoelectric Ceramics, Academic Press, New York, 1971.
[5] R.E. Eitel, C.A. Randall, T.R. Shrout, P.W. Rehrig, W. Hackenberger, S.E. Park, New high temperature morphotropic phase boundary piezoelectrics based on $Bi(Me)O_3$–$PbTiO_3$ ceramics, Japanese Journal of Applied Physics 40 (2001) 5999–6002.
[6] R.E. Eitel, C.A. Randall, T.R. Shrout, S.E. Park, Preparation and characterization of high temperature perovskite ferroelectrics in the solid-solution $(1 - x)BiScO_3$–$xPbTiO_3$, Japanese Journal of Applied Physics 41 (2002) 2099–2104.
[7] I. Sterianou, I.M. Reaney, D.C. Sinclair, D.I. Woodward, D.A. Hall, A.J. Bell, T.P. Comyn, High-temperature $(1 - x)BiSc_{1/2}Fe_{1/2}O_3$–$xPbTiO_3$ piezoelectric ceramics, Applied Physics Letters 87 (2005) 242901.
[8] I. Sterianou, D.C. Sinclair, I.M. Reaney, T.P. Comyn, A.J. Bell, Investigation of high curie temperature $(1 - x)BiSc_{1-y}Fe_yO3$–$xPbTiO_3$ piezoelectric ceramics, Journal of Applied Physics 106 (2009) 084107.
[9] H. Wen, X.H. Wang, X.Y. Deng, L.T. Li, Characterization of (1 0 0)-oriented $BiScO_3$–$PbTiO_3$ thin films synthesized by a modified sol–gel method, Applied Physics Letters 88 (2006) 222904.
[10] J.Z. Xiao, A.Y. Wu, P.M. Vilarinho, Sol–gel derived morphotropic phase boundary $0.37BiScO_3$–$0.63PbTiO_3$ thin films, Applied Physics Letters 92 (2008) 032902.
[11] T. Yoshimura, S. T-Mckinstry, Growth and properties of (0 0 1) $BiScO_3$–$PbTiO_3$ epitaxial films, Applied Physics Letters 81 (2002) 2065–2066.
[12] H. Wen, X.H. Wang, C.F. Zhong, L.K. Shu, L.T. Li, Epitaxial growth of sol–gel derived $BiScO_3$–$PbTiO_3$ thin film on Nb-doped $SrTiO_3$ single crystal substrate, Applied Physics Letters 90 (2007) 202902.
[13] H. Wen, X.H. Wang, X.Y. Deng, L.T. Li, Fabrication and properties of sol–gel derived $BiScO_3$–$PbTiO_3$ thin films, Journal of the American Ceramic Society 89 (2006) 2345–2347.
[14] F. Xu, S. Trolier-McKinstry, W. Ren, Xu Baomin, Z.-L. Xie, K.J. Hemker, Domain wall motion and its contribution to the dielectric and piezoelectric properties of lead zirconate titanate films, Journal of Applied Physics 89 (2001) 1336–1348.
[15] M. Algueró, H. Amorín, T. Hungría, J. Galy, A. Castro1, Macroscopic ferroelectricity and piezoelectricity in nanostructured $BiScO_3$–$PbTiO_3$ ceramics, Applied Physics Letters 94 (2009) 012902.
[16] X.Y. Deng, X.H. Wang, H. Wen, L.L. Chen, L. Chen, L.T. Li, Ferroelectric properties of nanocrystalline barium titanate ceramics, Applied Physics Letters 88 (2006) 252905.